Lithium-ion battery remaining useful life prediction with Box–Cox transformation and Monte Carlo simulation

YongZhi Zhang, *Student Member, IEEE*, Rui Xiong, *Senior Member, IEEE*, HongWen He, *Senior Member, IEEE*, and Michael Pecht, *Fellow, IEEE*

***Abstract*—The current lithium-ion battery remaining useful life (RUL) prediction techniques are mainly developed dependent on offline training data. The loaded current, temperature, and state of charge of lithium-ion batteries used for electric vehicles (EVs) change dramatically under the working conditions. Therefore, it is difficult to design acceleration aging tests of lithium-ion batteries under similar working conditions as those for EVs and to collect effective offline training data. To address this problem, this paper developed a RUL prediction method based on the Box–Cox transformation (BCT) and Monte Carlo (MC) simulation. This method can be implemented independent of offline training data. In the method, the BCT was used to transform the available capacity data and to construct a linear model between the transformed capacities and cycles. The constructed linear model using the BCT was extrapolated to predict the battery RUL, and the RUL prediction uncertainties were generated using the MC simulation. Experimental results showed that accurate and precise RULs were predicted with errors and standard deviations within, respectively, [–20, 10] cycles and [1.8, 7] cycles. If some offline training data is available, the method can reduce the required online training data and thus the acceleration aging test time of lithium-ion batteries. Experimental results showed that the acceleration time of the tested cells can be reduced by 70%-85% based on the developed method, which saved 1-3 months' acceleration test time compared to the particle filter method.**

***Index Terms*—Lithium-ion battery; Electric vehicles; Remaining useful life; Box-Cox transformation; Monte Carlo simulation; Acceleration aging test.**

This work was supported in part by the National Natural Science Foundation of China (Grant No. 51507012), Beijing Municipal Natural Science Foundation (Grant No. 3182035), and the Chinese Scholarship Council (CSC) [2016] 3100. The systemic experiments of the lithium-ion batteries were performed at the Advanced Energy Storage and Application (AESA) Group, Beijing Institute of Technology. (*Corresponding author: R. Xiong*)

Y. Zhang is with the National Engineering Laboratory for Electric Vehicles, Department of Vehicle Engineering, School of Mechanical Engineering, Beijing Institute of Technology, Beijing, 100081, China. He is also with the Center for Advanced Life Cycle Engineering (CALCE), University of Maryland, College Park, MD 20742, USA (yzzhangbit@gmail.com).

R. Xiong and H. He are with the National Engineering Laboratory for Electric Vehicles, Department of Vehicle Engineering, School of Mechanical Engineering, Beijing Institute of Technology, Beijing, 100081, China (rxiong@bit.edu.cn, hwhebit@bit.edu.cn).

M. Pecht is with the Center for Advanced Life Cycle Engineering (CALCE), University of Maryland, College Park, MD 20742, USA (pecht@umd.edu).

I. Introduction

LITHIUM-ION batteries are the main power sources of electric vehicles (EVs) [1-4]. The lifetime of lithium-ion batteries for EVs must be as long as or longer than that of EVs. However, owing to current manufacturing technology, lithium-ion batteries for EVs can reach their end of life (EOL) earlier than intended because of the dramatically changing working conditions. Generally, a battery reaches EOL when the capacity degrades more than 80% of its initial value [5]. Therefore, advanced techniques need to be developed to predict the remaining useful life (RUL) of lithium-ion batteries for EVs, so that users can replace the batteries in advance.

Lithium-ion battery RUL prediction has been performed mainly using model-based and data-driven methods. The model-based methods are generally implemented to predict the battery RUL based on a nonlinear aging model combined with an advanced filter technique such as particle filter (PF). Saha et al. [6] developed a Bayesian learning framework for battery RUL prediction. In the framework, the relevance vector machine (RVM) was used to extract features from the electrochemical impedance spectroscopy (EIS) to construct the aging model, and the PF method was used to update model parameters and predict the battery RUL. Because EIS can only be conducted offline, the developed methodology [6] is limited to offline applications. To address this limitation, He et al. [7] developed a method for battery RUL prediction using the Dempster-Shafer theory and the Bayesian Monte Carlo (BMC) method, which is also known as the PF method. Model parameters were initialized offline by combining sets of training data based on the Dempster–Shafer theory. BMC was then used to update the model parameters and predict the RUL based on the available data through online monitoring of the battery capacity. Based on the methodology of Ref. [7], a series of papers, including Xing et al. [8], Miao et al. [9], Liu et al. [10], and Su et al. [11], were published to either improve the aging model accuracy [8] or the filtering performance [9-13] for a more accurate RUL prediction. Dong et al. [12] used support vector regression (SVR)-PF to predict battery RUL, in which the particle degeneracy of PF was avoided by introducing SVR to rebuild a posterior distribution for resampling. Zheng et al. [13] developed a RUL prediction method using unscented Kalman filter (UKF) with relevance vector regression (RVR). The RVR was employed as a nonlinear time-series prediction model to predict the UKF future residuals for model parameter update and battery RUL prediction purposes.

The model-based prognostic method requires the online cell to work under the same conditions as the offline cells, so that an accurate nonlinear aging model can be initialized based on the offline training data. A sufficient amount of online capacity degradation data is also required to initialize an accurate RUL predictor. The typical amount of online data for the model

This article has been accepted for publication in a future issue of this journal, but has not been fully edited. Content may change prior to final publication. Citation information: DOI 10.1109/TIE.2018.2808918, IEEE Transactions on Industrial Electronics

parameter initialization accounts for 40%-70% of the complete degradation data [6-13]. In this paper, the offline cell refers to the cell whose degradation data is completely obtained and considered as the training data, whereas the online cell refers to the cell whose degradation data is only partially known and its RUL needs to be predicted. The online cells can refer to the on-board cells or testing cells.

The data-driven methods for battery RUL prediction depend on machine learning techniques. Nuhic et al. [14] used the support vector machine (SVM) to embed diagnosis and prognostics of system health with an aim to estimate the state of health (SOH) and RUL of lithium-ion batteries. Patil et al. [15] proposed a multistage SVM approach for RUL prediction of lithium-ion batteries. This approach integrated classification and regression attributes of SVM, in which the classification model provided a gross estimation and the regression model was used to predict the RUL. Liu et al. [16] employed the Box–Cox transformation (BCT) to build a relationship between the extracted features and capacities of lithium-ion batteries, and the relevance vector machine (RVM) was then used to predict RUL based on the extracted features. Besides the kernel techniques [14-16], neural network (NN) techniques were also employed to predict the RUL of lithium-ion batteries. Liu et al. [17] proposed an adaptive recurrent neural network (ARNN) for system dynamic state forecasting for the purpose of predicting the RUL of lithium-ion batteries. Based on degradation data of lithium-ion batteries from NASA, Liu et al. [17] validated that the ARNN showed better learning capability than classical training algorithms, including the recurrent neural network (RNN) and RVM methods. Compared with model-based methods, machine learning techniques usually need a large amount of offline training data to construct an accurate online RUL predictor.

The conventional lithium-ion battery RUL prediction techniques [6-17] generally depend on offline training data. These techniques can be used when the online cell works in stable charging/discharging conditions, such as portable electronics, including cell phones and laptops, and the required offline data under similar working conditions can thus be collected by performing acceleration aging tests. However, the working conditions of lithium-ion batteries for EVs, including the loaded current, temperature, and state of charge (SOC), are dramatically changeable. Therefore, it is difficult to design acceleration aging tests for lithium-ion batteries to collect effective offline training data under the similar working conditions as those for EVs. The conventional methods are not applicable to battery RUL predictions for EVs. To address this problem, a RUL prediction method based on the BCT and Monte Carlo (MC) simulation was developed. The main advantage of this method is that it is capable of predicting the battery RUL independent of offline training data. Another advantage of the developed method is that it can reduce the required online data for accurate RUL prediction by combining the offline training data. This feature can reduce the acceleration aging test time of lithium-ion batteries, which usually takes more than six months to reach the battery EOL depending on the specific test conditions. The human and material resources can be reduced because three or more cells are usually tested under the same conditions. It is efficient to predict the cell's EOL at an early life stage based on the capacity data of other cells that have reached the EOL under the same test condition.

The rest of this paper is organized as follows: Section 2 presents the battery testing conditions and the capacity degradation data. Section 3 describes the algorithms for the battery RUL prediction, followed by the implementation process introduced in Section 4. Section 5 presents the RUL prediction results based on the developed method, and Section 6 concludes the paper.

II. Battery Testing and Degradation Data

To investigate the aging characteristics of lithium-ion batteries, high-energy 18650 lithium-ion batteries manufactured by Panasonic, labeled NCR18650PF, were used. The cells had a rated capacity of 2.7 Ah. The nominal voltage was 3.6 V, with the upper and lower cut-off voltages being 4.2 V and 2.5 V, respectively. The materials consisted of graphite on the anode and $Li(NiCoAl)O_2$ on the cathode.

The cell test conditions are summarized in Table 1. For illustration purposes, the six tested cells are labeled A to F. In the cycling test, the charging profile of all cells is a constant current (CC)-constant voltage (CV) process with a constant current rate of 0.5C, followed by a constant voltage of 4.2 V, and the cut-off current rate is 0.05 C. The cells were, respectively, discharged under 0.5C, 1C, and 2C current rates until the low cut-off voltage was reached, then a 0.5C current rate was loaded on all cells until the low cut-off voltage was reached again. In this paper, the battery was considered to reach the 0% SOC level when it was discharged until the low cut-off voltage under a 0.5C rate. The 0.5C current loaded on the battery at the end of discharging was to discharge the remaining charges, and to ensure that the batteries under different discharge current rates were discharged to the same low SOC level (0% SOC). The capacity used to indicate battery degradation was obtained by accumulating all the discharged capacities. The rest time between charging and discharging was 30 min. The degradation trajectories of the battery capacity under each condition are presented in Fig. 1. At $T = 10$ °C, Cells A and B were, respectively, discharged under 0.5C and 1C current rates. Cells C and D were, respectively, discharged under 1C and 2C current rates at $T = 25$ °C, whereas Cells E and F were, respectively, discharged under 1C and 2C current rates at $T = 40$ °C. To reduce the acceleration test time, Cells A and B were only experimented under the cycle test. The characteristic tests, including the capacity calibration test, the dynamic stress test (DST), and the open circuit voltage (OCV) test, were conducted on Cells C–F every 50 or 100 cycles. The characteristic tests were conducted for battery aging characteristic analysis, and the test data was not utilized in this paper. Under each test condition, two or four cell samples were

Table 1 Cell test conditions of the NCR18650PF battery

Test condition	Cells A-B	Cells C-D	Cells E-F
Cycle test	Charge: CCCV, charged at 0.5C rate up to 4.2V 0.05C rate-cutoff Charge rest: 30 min Discharge: 0.5C rate (Cell A) and 1C rate (Cell B), 2.5V-cutoff Discharge rest: 30 min Temperature: 10 °C	Charge: CCCV, charged at 0.5C rate up to 4.2V 0.05C rate-cutoff Charge rest: 30 min Discharge: 1C rate (Cell C) and 2C rate (Cell D), 2.5V-cutoff Discharge rest: 30 min Temperature: 25 °C	Charge: CCCV, charged at 0.5C rate up to 4.2V 0.05C rate-cutoff Charge rest: 30 min Discharge: 1C rate (Cell E) and 2C rate (Cell F), 2.5V-cutoff Discharge rest: 30 min Temperature: 40 °C
Characteristic test	-	Capacity calibration-OCV test-DST test	Capacity calibration-OCV test-DST test

This article has been accepted for publication in a future issue of this journal, but has not been fully edited. Content may change prior to final publication. Citation information: DOI 10.1109/TIE.2018.2808918, IEEE Transactions on Industrial Electronics

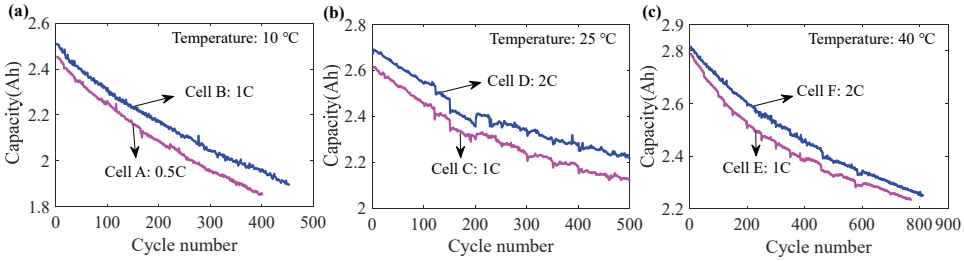

Fig. 1 Capacity degradation trajectories of battery at different currents and temperatures: (a) Cell A under 0.5C and Cell B under 1C with T = 10 °C; (b) Cell C under 1C and Cell D under 2C with T = 25 °C; (c) Cell E under 1C and Cell F under 2C with T = 40 °C.

used. Cells A, C, and E were, respectively, the ones selected from four cells while Cells B, D, and F were, respectively, the ones selected from two cells. For Cells A and B, the EOL threshold was set to 75% of their respective initial capacities, whereas for Cells C–F, the EOL threshold was set to 80% of their respective initial capacities.

Fig. 1 shows a lower convex degradation trend of capacity with the capacity degradation rate decreasing as the battery ages. This category of capacity degradation trend can be observed in batteries such as the Li(NiCoAl)O_2 or $LiCoO_2$ based batteries [18, 19]. There are also some batteries, such as the $LiMn_2O_4$ or $LiFePO_4$ based batteries, showing an upper convex degradation trend of capacity [7, 20, 21]. In this case, a fast degradation rate of capacity can occur at the battery EOL. The method in this paper was specifically developed for the RUL prediction of batteries with a lower convex degradation trend of capacity as shown in Fig. 1.

The experimental data of battery aging tests was used to evaluate the performance of the developed battery RUL prediction method for EVs. Although the lithium-ion batteries for EVs work under dramatically changeable currents, temperatures, and SOCs, the capacity degradation trends are expected to follow lower convex degradations as shown in Fig. 1 under different working conditions. Therefore, the verification results of the developed method based on capacity data of Fig. 1 can be used to evaluate its application performance for EVs. The battery EOLs and slope sizes of capacity degradation at the battery EOL in Fig. 1 are different under different working conditions. The RUL prediction accuracy is highly dependent on the capacity prediction results at the battery EOL. The differences of battery EOLs and slope sizes of capacity degradation at the battery EOL can decrease the battery RUL prediction accuracy for the traditional methods, which perform RUL predictions dependent on offline training data under working conditions different than the online cells. Since it is difficult to collect effective offline training data of batteries under the same working conditions as EVs, there is a need to develop RUL prediction methods independent of offline training data.

III. Algorithms

This section introduces the algorithms for lithium-ion battery RUL predictions, including the BCT, the least squares algorithm and the MC simulation.

A. Box–Cox transformation

The current battery RUL prediction techniques are mainly developed using nonlinear aging models such as the two-term exponential aging model [7]. To describe the battery capacity degradation accurately, there are generally more than four parameters of the nonlinear aging models [6-11] to be identified. It is difficult to identify these model parameters accurately without learning the complete degradation data. This is why the offline training data is required to initialize the nonlinear aging model for an accurate RUL prediction. BCT is able to transform a nonlinear degradation into a linear degradation with only one parameter to be identified and the offline training data is thus not required. This paper utilizes the BCT to transform the capacity degradation trends of lithium-ion batteries to improve the RUL prediction performance, which is different from the application in Ref. [16], where BCT was used for fitting purposes.

BCT is a parametric power transformation technique that improves additivity, normality, and homoscedasticity of observations. Herein, the observations represent the collected capacities. The BCT, as originally appeared in Ref. [22], takes the following form for $y > 0$

$$y(\lambda)=\begin{cases}\dfrac{y^{\lambda}-1}{\lambda}, & \lambda\neq 0\\ \log y, & \lambda=0\end{cases} \tag{1}$$

where y represents the observation, and λ is the transformation parameter to be identified. The aim of BCT is to ensure the usual assumptions for linear model hold, which is $\boldsymbol{y}(\lambda)\sim N(\boldsymbol{X\beta},\boldsymbol{\sigma^2})$ and can be expressed as

$$\begin{cases} y_i(\lambda)=\beta_0+x_{i1}\beta_1+x_{i2}\beta_2+\ldots+x_{im}\beta_m+\varepsilon_i\\ \varepsilon_i=N\left(0,\sigma^2\right),\ i=1,2,\ldots,n\end{cases} \tag{2}$$

where $\boldsymbol{y}(\lambda)=(y_1(\lambda),y_2(\lambda),\ldots,y_n(\lambda))^T$, $\boldsymbol{X}$ is a design matrix with $\boldsymbol{X}=(\boldsymbol{X_1},\boldsymbol{X_2},\ldots,\boldsymbol{X_n})^{\boldsymbol{T}}$ and $\boldsymbol{X_i}=(1,x_{i1},x_{i2},\ldots,x_{im})$, $\boldsymbol{\beta}=(\beta_0,\beta_1,\beta_2,\ldots,\beta_m)^{\boldsymbol{T}}$, m is the number of independent variables, n is the sample size, $x_1,x_2,\ldots,x_m$ represent the battery aging related factors such as the cycle number, the working temperature, and the discharging current rate. $\beta_1,\beta_2,\ldots,\beta_m$ are the coefficients, and ε_i are random errors that are independent and normally distributed with a zero mean and variance of σ^2.

The maximum likelihood (ML) method [23] was utilized for identification of λ. Since the transformed responses $\boldsymbol{y}(\lambda)\sim N(\boldsymbol{X\beta},\sigma^2\boldsymbol{I})$, the joint probability density function of $\boldsymbol{y}(\lambda)$ is

$$f\left(\boldsymbol{y}(\lambda)\right)=\frac{\exp\left\{-\frac{1}{2\sigma^2}\left[\boldsymbol{y}(\lambda)-\boldsymbol{X\beta}\right]^T\left[\boldsymbol{y}(\lambda)-\boldsymbol{X\beta}\right]\right\}}{\left(2\pi\sigma^2\right)^{n/2}} \tag{3}$$

$J(\lambda,\boldsymbol{y})$ is assumed to be the Jacobian of the transformation from $\boldsymbol{y}$ to $\boldsymbol{y}(\lambda)$, and the joint probability density function of $\boldsymbol{y}$ is expressed as

$$f(\boldsymbol{y})=\frac{\exp\left\{-\frac{1}{2\sigma^2}\left[\boldsymbol{y}(\lambda)-\boldsymbol{X\beta}\right]^T\left[\boldsymbol{y}(\lambda)-\boldsymbol{X\beta}\right]\right\}}{\left(2\pi\sigma^2\right)^{n/2}}J(\lambda,\boldsymbol{y}) \tag{4}$$

where $J(\lambda,\boldsymbol{y})=\prod_{i=1}^{n}y_i^{\lambda-1}$.

The log-likelihood function from Eq. (4) can be expressed as

This article has been accepted for publication in a future issue of this journal, but has not been fully edited. Content may change prior to final publication. Citation information: DOI 10.1109/TIE.2018.2808918, IEEE Transactions on Industrial Electronics

$$L\left(\boldsymbol{\beta},\sigma^2,\lambda\middle|\boldsymbol{y},\boldsymbol{X}\right)=-\frac{n}{2}\log 2\pi-\frac{n}{2}\log\sigma^2-\frac{1}{2\sigma^2}\left[\boldsymbol{y}(\lambda)-\boldsymbol{X\beta}\right]^T\left[\boldsymbol{y}(\lambda)-\boldsymbol{X\beta}\right]+(\lambda-1)\sum_{i=1}^{n}\log(y_i) \quad (5)$$

Taking the partial derivatives of $L(\boldsymbol{\beta},\sigma^2,\lambda|\boldsymbol{y}(\lambda),\boldsymbol{X})$ with respect to $\boldsymbol{\beta}$ and σ^2 respectively, and setting each of the resulting equations to zeros yields

$$\hat{\boldsymbol{\beta}}(\lambda)=\left(\boldsymbol{X}^T\boldsymbol{X}\right)^{-1}\boldsymbol{X}^T\boldsymbol{y}(\lambda) \quad (6)$$

$$\hat{\sigma}^2(\lambda)=\frac{\left[\boldsymbol{y}(\lambda)-\boldsymbol{X\beta}\right]^T\left[\boldsymbol{y}(\lambda)-\boldsymbol{X\beta}\right]}{n} \quad (7)$$

Substituting $\hat{\boldsymbol{\beta}}(\lambda)$ and $\hat{\sigma}^2(\lambda)$ into Eq. (5) obtains the profile log-likelihood function for λ alone

$$L(\lambda)=C-\frac{n}{2}\log\left(\hat{\sigma}^2(\lambda)\right)+(\lambda-1)\sum_{i=1}^{n}\log(y_i) \quad (8)$$

where $C=-\frac{n}{2}\ln 2\pi-\frac{n}{2}$. To maximize Eq. (8), it is equivalent to maximizing the value of

$$L^*(\lambda)=\frac{n}{2}\log\left(\hat{\sigma}^2(\lambda)\right)+(\lambda-1)\sum_{i=1}^{n}\log(y_i) \quad (9)$$

After the value of $\hat{\lambda}$ is determined, $\hat{\boldsymbol{\beta}}$ can be calculated using the least squares algorithm.

B. Linear regression based on least squares algorithm

This paper constructs a linear model between the transformed capacities vs. cycles, so there is only one independent variable that represents the cycle number and thus $m=1$. In this case, Eq. (2) can be written as

$$\begin{cases} y_i(\lambda)=\beta_0+x_i\beta_1+\varepsilon_i \\ \varepsilon_i=N\left(0,\sigma^2\right),\ i=1,2,...,n \end{cases} \quad (10)$$

where n is the sample size, and x represents the cycle number. The fitted equation is defined as

$$\hat{y}_i(\lambda)=b_0+x_ib_1+\varepsilon_i \quad (11)$$

where $b_0=\hat{\beta}_0$, and $b_1=\hat{\beta}_1$. That is, for each observed response $y_i(\lambda)$, with a corresponding predictor variable x_i, a fitted value is obtained as Eq. (11). b_0 and b_1 can be estimated by minimizing the distance of the data points to the fitted line, which equivalents to minimizing the sum of squared residuals (SSR), where

$$SSR=\sum_{i=1}^{n}\left(y_i(\lambda)-\hat{y}_i(\lambda)\right)^2=\sum_{i=1}^{n}\left[y_i(\lambda)-\left(b_0+b_1x_i\right)\right]^2 \quad (12)$$

Taking partial derivatives of SSR with respect to b_0 and b_1 respectively, and setting each of the resulting equations to zero yields

$$\begin{cases} b_1=\dfrac{\sum_{i=1}^{n}\left(x_i-\bar{x}\right)\left(y_i(\lambda)-\bar{y}(\lambda)\right)}{\sum_{i=1}^{n}\left(x_i-\bar{x}\right)^2} & (13) \\ b_0=\bar{y}(\lambda)-b_1\bar{x} & (14) \end{cases}$$

where $\bar{x}=\frac{\sum_{i=1}^{n}x_i}{n}$, and $\bar{y}(\lambda)=\frac{\sum_{i=1}^{n}y_i(\lambda)}{n}$.

The variances of the coefficients b_0 and b_1 are, respectively, estimated as

$$\begin{cases} Var(b_1)=\dfrac{s^2}{\sum_{i=1}^{n}\left(x_i-\bar{x}\right)^2} & (15) \\ Var(b_0)=s^2\left[\dfrac{1}{n}+\dfrac{\bar{x}^2}{\sum_{i=1}^{n}\left(x_i-\bar{x}\right)^2}\right] & (16) \end{cases}$$

where s^2 represents the estimate of σ^2 of the error term and is estimated as $s^2=SSR/(n-2)$. Readers can refer to Ref. [24] for formula derivation details of Eqs. (12)-(16).

The Pearson correlation analysis [25] can be used to quantitatively evaluate the linear relationship between the independent variable x and observation y. The Pearson correlation coefficient is computed as

$$r=\frac{\sum_{i=1}^{n}\left(x_i-\bar{x}\right)\left(y_i-\bar{y}\right)}{\sqrt{\sum_{i=1}^{n}\left(x_i-\bar{x}\right)^2}\sqrt{\sum_{i=1}^{n}\left(y_i-\bar{y}\right)^2}} \quad (17)$$

where r is between -1 and $+1$, and a perfect linear relationship exists between the independent variable x and observation y when the correlation coefficient $r=\pm 1$. $r=0$ indicating no linear relationship between x and y exists.

C. Monte Carlo simulation

MC simulation is able to propagate the input uncertainties into prediction uncertainties [26]. In MC simulation, the system is generally simulated ~10^3-10^6 times [27]. Each simulation amounts to a realization of the system. For each realization, all of the uncertain parameters are sampled based on the specified distribution that describes each parameter. Given the particular set of input parameters, the system is simulated through time such that the performance of the system can be computed. MC simulation leads to many separate and independent realizations of the system, with each representing the possible evolution characteristics of the system through time. These realizations make up the probability distributions of possible outcomes.

When constructing a model for MC simulation, the uncertainties that describe model parameters are generally obtained based on the statistics of historical data. Beer et al. [28] trained a neural network based on the observed data, and the trained network was then applied to generate a set of random process realizations which reflected the properties of the training data. In Ref. [29], a stochastic-heuristic methodology for the optimization of the electric supply of off-grid hybrid systems was developed. The stochastic optimization was developed by means of MC simulation, which took into account the uncertainties of irradiation, temperature, wind speed, and load and used the PDFs that were generated from the historical data. In this paper, the parameter uncertainties are generated in the linear regression process.

IV. Implementation

The developed method was used to predict the battery RUL based on the available capacity data. The BCT was applied to construct a linear relationship between the transformed capacities and cycles, which is expressed as

$$\begin{cases} C_i(\lambda)=\beta_0+k_i\beta_1+\varepsilon_i \\ \varepsilon_i=N\left(0,\sigma^2\right),\ i=1,2,...,n \end{cases} \quad (18)$$

where $C(\lambda)$ represents the transformed battery capacity using the BCT, and k represents the cycle number referring to a corresponding capacity value. Eq. (18) has the same form as Eq.

This article has been accepted for publication in a future issue of this journal, but has not been fully edited. Content may change prior to final publication. Citation information: DOI 10.1109/TIE.2018.2808918, IEEE Transactions on Industrial Electronics

(10), and the developed method can thus be used to identify the model parameters.

Figure 2 shows the framework of lithium-ion battery RUL predictions for EVs based on the developed method, which includes four steps. Step 1 uses the BCT to transform the collected capacity data and to construct a linear aging model expressed as Eq. (18), which describes the linear relationship of the transformed capacity $C(\lambda)$ vs. the cycle k. Step 2 uses the least squares algorithm to identify the model parameters. The parameterized aging model in Step 2 can be extrapolated to predict the battery EOL without providing prediction uncertainties. However, the confidence intervals of lithium-ion battery RUL predictions are required for making an economic maintenance strategy of batteries in practice. Therefore, Step 3 uses the MC simulation to generate 10^3 sets of model parameters based on the parameter variances (Eqs. (15)-(16)). The aging model with each model parameter set is extrapolated to make multiple-step-ahead predictions in Step 4, and when the predicted capacity is lower than the threshold, an EOL is reported. There are 10^3 predicted RULs for each prediction, which can be used to generate the RUL prediction uncertainties. Note that the developed framework in Fig. 2 is not limited to the lithium-ion battery RUL prediction for EVs, and can be used to predict the battery RUL for electronics including cell phones and laptops.

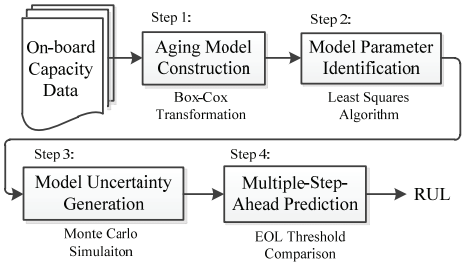

Fig. 2 Framework of lithium-ion battery RUL prediction for EVs.

Figure 3 shows the RUL prediction results of Cells C and D by using the developed method, in which the RUL prediction results based on two nonlinear models are also presented as comparisons. These two nonlinear aging models, which include the second-order polynomial as a simple model [8] and the two-term exponential as a complicated model [7], are commonly used for describing the capacity degradations of lithium-ion batteries. The simulation was implemented on a laptop equipped with an Intel Core i7-6700 HQ processor (6 MB cache, up to 3.50 GHz) using Matlab R2016b software. In Figs. 3(a-b), the estimated values of the transformation parameter λ are, respectively, –6.53 and –8.72 when the BCT is applied to transform the complete degradation data of Cells C and D, and these λ values are, respectively, considered the λ references of Cells C and D in this paper. Fig. 3(a) shows the RUL prediction results of Cell C based on the capacity data of previous 300 cycles, in which the Matlab-based simulation time is 2.25 s. The estimated λ based on the data of previous 300 cycles is –6.80, which is 0.27 smaller than the λ reference. The estimated λ is used to transform the real data to obtain the transformed capacities, and a linear model describing the relationship of the transformed capacity $C(\lambda)$ vs. cycle k before 300 cycles is constructed. The Pearson correlation coefficient r is –0.9888, indicating a strong linear relationship of $C(\lambda)$ vs. k. The linear model is then extrapolated to make multiple-step-ahead predictions and when the predicted value is lower than the threshold, an EOL is reported. There is one EOL prediction for each Monte Carlo simulation, and the simulation is repeated 10^3 times in this paper. The mean value of predicted EOLs is 505 cycles, which is 5 cycles larger than the real EOL. The standard deviation is 5 cycles, and the 95% confidence bound is thus [495, 515]. Fig. 3(b) shows the RUL prediction results of Cell D, in which the capacity data of previous 310 cycles is used to predict the cell EOL using the developed method. The Matlab-based simulation time is 2.35 s. The λ estimate of the BCT based on the capacity data of previous 310 cycles is –7.19, which is 1.53 larger than the reference value. The Pearson correlation coefficient r of the transformed capacities of previous 300 cycles vs. cycles is –0.9769, indicating a strong linear relationship of $C(\lambda)$ vs. k. The predicted EOL is 488 cycles, which is 12 cycles smaller than the real EOL. The standard deviation is 7 cycles, and the 95% confidence bound is thus [474, 502]. In Fig. 3(c), the previous 300 cycles' capacities were used to fit the polynomial and exponential using the curve fitting tool of Matlab, and the capacities after 300 cycles were predicted by extrapolating the nonlinear models. The polynomial and exponential prediction capacities decreased a little at first and then increased as the cycle number increased, which moved farther away from the real capacities as the cycle number increased. Therefore, the nonlinear models fail to predict an EOL for Cell C. Fig. 3(d) shows similar capacity prediction results as those in Fig. 3(c), in which the nonlinear models fail to catch the capacity degradations for battery RUL predictions.

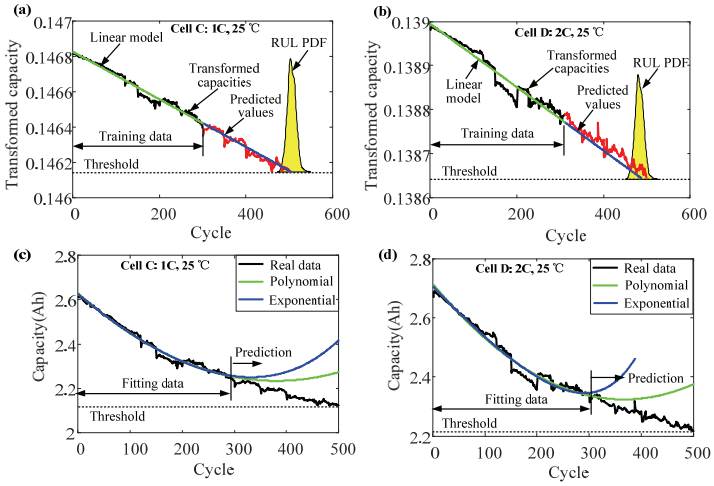

Fig. 3 RUL prediction results: (a-b) based on the developed method; and (c-d) based on nonlinear models.

This article has been accepted for publication in a future issue of this journal, but has not been fully edited. Content may change prior to final publication. Citation information: DOI 10.1109/TIE.2018.2808918, IEEE Transactions on Industrial Electronics

The time required by the developed method to predict accurate and precise RULs for Cells C and D based on Matlab varies around 2.3 s. This time is expected to be longer in practice, which can be a few minutes owing to the lower performance of the central processing unit (CPU) of the battery management system used for EVs than that of the computer. However, it generally takes several hours or several days to complete one cycle of charging/discharging for lithium-ion batteries of EVs. Therefore, the developed method can realize on-board battery RUL predictions for EVs efficiently. The failure in RUL predictions by replacing the BCT with nonlinear models indicates the effectiveness and superiority of the BCT compared to the nonlinear models.

V. Results

To evaluate its effectiveness and performance, the developed method was applied for predicting the battery RUL based on experimental data of 15 cells under different currents and temperatures. Herein, the prognostic robustness of the developed method against erroneous transform parameters was firstly analyzed. Then, the developed method was performed for battery RUL predictions in two cases: in one case, no offline training data was available, whereas in another case, some offline training data was available.

A. Robustness against erroneous transform parameters

The transform parameter λ decides the linear relationship of the transformed capacities vs. cycles, and the RUL prediction accuracy is based on this relationship. In practice, the λ reference is usually unavailable since the BCT can only be implemented on the data we have rather than the complete degradation data of the cell. Generally, the estimated value of λ based on the collected degradation data is biased from the reference. Therefore, it is necessary to evaluate the RUL prediction robustness of the developed method against erroneous λ values. Figure 4 shows the RUL prediction errors with erroneous transform parameters of different cells. The λ reference of each cell is obtained based on the complete degradation data of the cell. The negative λ error indicates a lower λ than the reference whereas the positive λ error indicates a larger λ than the reference. A λ error of zero indicates that the λ is equal to the reference. The λ is applied to transform the available capacity data to construct a liner relationship between the transformed capacities and cycles. The lithium-ion battery RUL is then predicted dependent on the extrapolation of this linear relationship. For each cell and each given λ value, the RUL prediction starts when 20% of the complete degradation data of the cell is available and operates every 10 cycles until the cell EOL. In each case, the expectation and 95% confidence bounds are obtained based on all RUL prediction errors at the specified started cycles. Fig. 4 shows the expectation, the 95% lower confidence bound and upper confidence bound of each cell with a λ error from –2 to 2. The negative RUL error indicates a delayed RUL prediction, whereas the positive RUL error indicates an advanced RUL prediction. Generally, the RUL error is linearly and positively related to the λ error, and a negative λ error corresponds to a delayed RUL prediction, whereas a positive λ error corresponds to an advanced RUL prediction. The lowest RUL error, which is close to zero, occurs when the λ error is zero for each cell except Cell D. For Cell D, the lowest RUL error exists at a λ error of 1.5, and when the λ error is 0, a delayed RUL error of about –40 is observed. However, the maximum absolute RUL error of Cell D, which is about 100 cycles at a λ error of –2, is similar to those of other cells except that of Cell C, whose absolute value is about 40 cycles at the same λ error point. The 95% confidence bounds, which indicate the RUL prediction robustness against different starting cycles, all shorten as the λ error moves closer to zero except Cell D, whose 95% confidence bounds increase a little as the λ error decreases from 2 to 0. To obtain accurate and robust RUL predictions against erroneous λ values for all cells, the λ error margin is set at [–1, 2]. That is, the RUL prediction is considered accurate and robust as the λ error falls within [–1, 2], where the RUL prediction errors are within [–50, 50] cycles, and the 95% confidence bounds are within 10 cycles of most cells. This error margin of λ for accurate RUL predictions indicate a high prediction stability of the developed method.

The reason that a RUL prediction error of about –40 cycles is observed at the zero λ error point of Cell D can be explained according to Fig. 5. Fig. 5 shows the RUL prediction results of Cell D using the λ reference value of –8.72. The x-axis in Fig. 5 indicates the starting cycle for RUL prediction, and at each starting cycle, the available capacities are transformed using the BCT based on the λ reference so that a linear aging model describing the relationship of transformed capacities and cycles is constructed. The linear aging model is extrapolated to predict the RUL. When the capacities of Cell D are all transformed using the BCT based on the λ reference, the Pearson correlation coefficient of the transformed capacities and cycles is –0.9922, indicating a strong linear relationship. Fig. 5 shows that when the RUL is predicted at 100–150 cycles, the RUL prediction

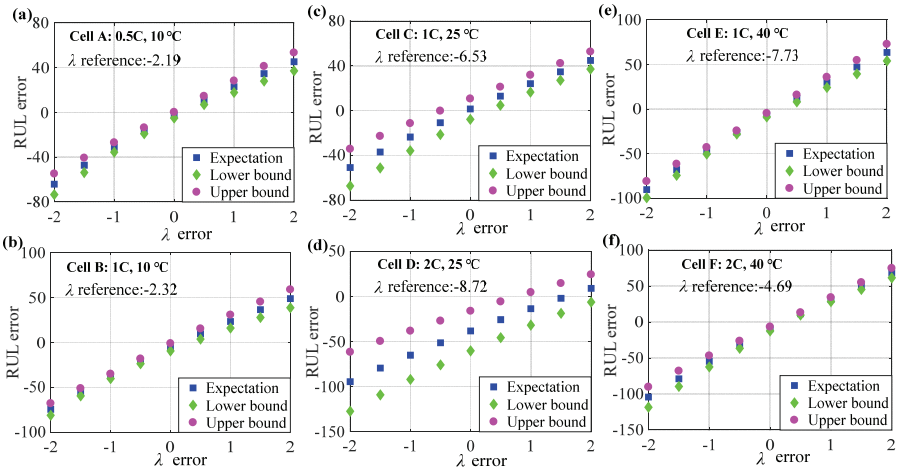

Fig.4 RUL prediction error with erroneous transform parameters of: (a) Cell A; (b) Cell B; (c) Cell C; (d) Cell D; (e) Cell E; (f) Cell F.

This article has been accepted for publication in a future issue of this journal, but has not been fully edited. Content may change prior to final publication. Citation information: DOI 10.1109/TIE.2018.2808918, IEEE Transactions on Industrial Electronics

errors vary around –200 cycles, which contributes about a half to the predicted expectation error in Fig. 4(d) at the zero λ error point. After 150 cycles, the RUL prediction errors drop sharply and then mainly varies around –20 cycles, which contributes another half to the expectation error. The large prediction variations caused by the predictions at 100–150 cycles lead to a wider 95% confidence bound in Fig. 4(d) at the λ error point of zero than those in other Figs. The 95% confidence bound of the RUL prediction error after 150 cycles is 16 cycles. Therefore, an accurate and robust RUL of Cell D can still be predicted with a λ error within [–1, 2] when more than 150 cycles' capacities are available. The analysis results can be used for explaining the large RUL prediction errors of Cell D obtained in other cases when the λ error is not zero.

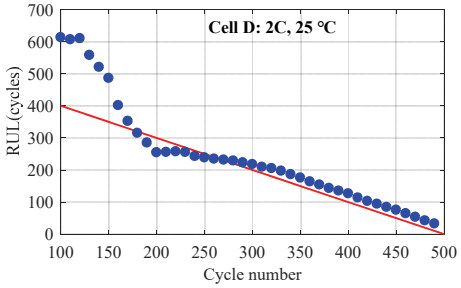

Fig.5 RUL prediction results of Cell D based on the λ reference.

B. Remaining useful life prediction without offline training data

Figure 6 shows the RUL prediction results of Cells A and B using BCT. The BCT was applied to transform the available capacity degradation data, and the RUL was then predicted based on the extrapolation of the linear relationship between the transformed capacities and cycles. The BCT was applied to transform the capacity data of each cell at a started cycle of 50, and then operated every 10 cycles until the cell EOL. Figs. 6(a-c) show the prediction results of Cell A. Fig. 6(a) shows the λ estimate at different cycles of Cell A, where the λ reference was obtained based on the complete degradation data of Cell A. The lower and upper thresholds represent the λ error margin with an accurate and robust RUL prediction, and are, respectively, –1 lower and 2 larger than the reference. The λ estimate is far away from the reference at the beginning but converges to the reference as more degradation data is available. The λ estimate falls within the λ error margin at 170 cycles, where the RUL prediction starts and the prediction result is shown in Fig. 6(b). The predicted RUL is close to the real value and the absolute RUL prediction errors vary within 10 cycles at most cycles. The RUL prediction error shows a similar changing trend as the λ estimation error. The more accurate the λ estimate is, the closer the predicted RUL is to the real RUL. Usually, a negative λ error leads to a delayed RUL prediction, whereas a positive λ error leads to an advanced RUL prediction. Fig. 6(c) shows the standard deviation (STD) of the RUL prediction at the specified cycles. The STD was obtained using the MC simulation. The RUL prediction is precise with all STDs within 3 cycles, and the STD decreases as more degradation data is available, indicating a more precise RUL prediction. Figs. 6(d-f) show the RUL prediction results of Cell B. The λ estimate falls within the error margin at 280 cycles. At most cycles, the predicted RUL is close to the real value with a prediction error less than 15 cycles. The STDs of the RUL predictions are all within 2 cycles and decrease as more degradation data is available.

Figure 7 shows the RUL prediction results of Cells C and D, where Figs. 7(a-c) show the prediction results of Cell C and Figs. 7(d-f) show the prediction results of Cell D. The λ estimates of Cells C and D both fluctuate at the beginning and converge to the references after 180 cycles. The estimated λ of Cells C and D falls within the error margin at 250 and 310 cycles, respectively. Still, the predicted RUL shows the same changing trend as the λ estimate. The predicted RUL of Cell C converges to the real value from an error of about 60 cycles. Once converging to the real value, the predicted RUL is accurate and close to the real RUL with prediction errors within ± 10 cycles at most cycles. The RUL predictions of Cell D are close to the real values with errors varying around –20 cycles at most cycles. At different cycles, the STDs of the RUL predictions of Cell C are within 6 cycles while those of Cell D are within 7 cycles, and the STDs of both Cells C and D decrease as more degradation data is available.

Figure 8 shows the RUL prediction results of Cells E and F, where Figs. 8(a-c) show the prediction results of Cell E and Figs. 8(d-f) show the prediction results of Cell F. The estimated λ of Cells E and F falls within the error margin at 200 and 110 cycles, respectively. The predicted RULs of Cells E and F both varies around the respective real values with RUL prediction errors being within ± 10 at most cycles. The RUL prediction errors of each cell show the same changing trend as the estimated λ varies around the λ reference. The STDs of Cell E are all less than 3.5 cycles, and although some variations are observed with more available degradation data, the STDs show a decreased

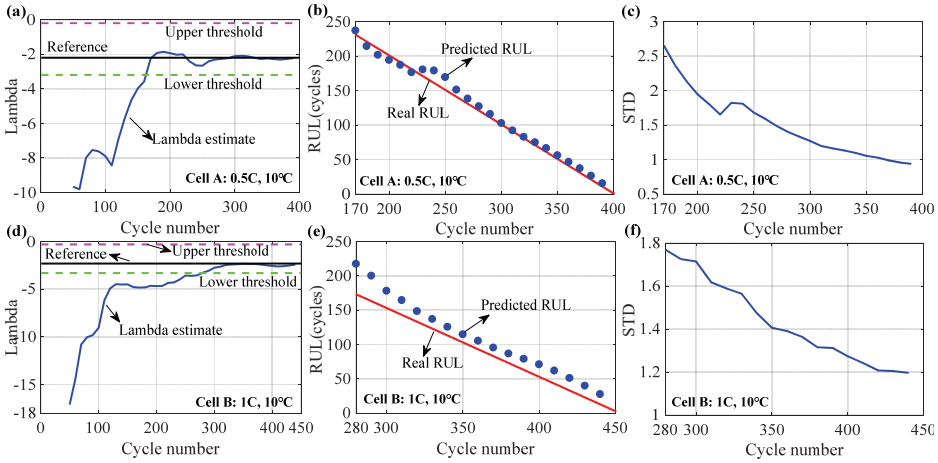

Fig. 6 RUL prediction results: (a) λ estimate of Cell A; (b) RUL prediction of Cell A; (c) STD of Cell A; (d) λ estimate of Cell B; (e) RUL prediction of Cell B; (f) STD of Cell B.

This article has been accepted for publication in a future issue of this journal, but has not been fully edited. Content may change prior to final publication. Citation information: DOI 10.1109/TIE.2018.2808918, IEEE Transactions on Industrial Electronics

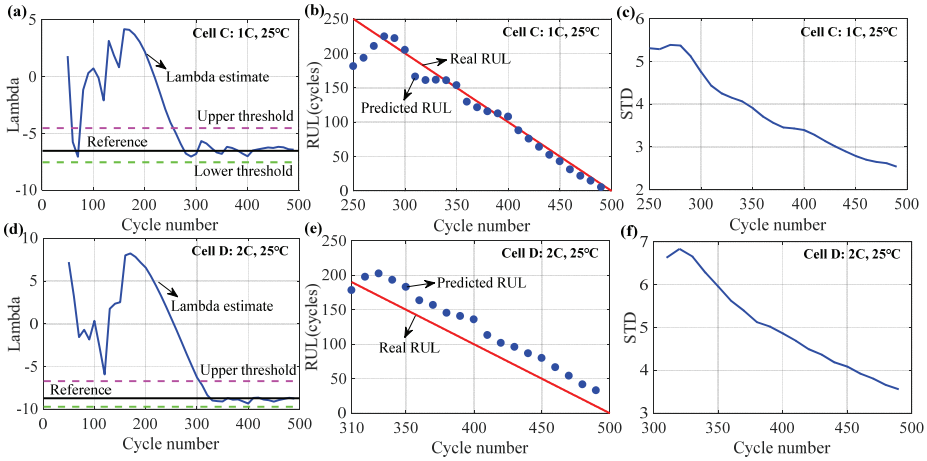

Fig. 7 Prediction results: (a) λ estimate of Cell C; (b) RUL prediction of Cell C; (c) STD of Cell C; (d) λ estimate of Cell D; (e) RUL prediction of Cell D; (f) STD of Cell D.

changing trend. The STDs of Cell F are within 7 cycles and decreases with more available data.

The BCT-based method is used to transform the online collected degradation data of previous cycles of the cell, and to build a linear relationship of transformed capacities vs. cycles for the RUL prediction. The RUL prediction starts when the estimated λ falls within the error margin. The starting cycles for accurate RUL predictions of Cells A–F are, respectively, 170, 280, 250, 310, 190, and 110 cycles, which cover 15%–60% of the complete data of different cells. When the estimated λ falls within the error margin, the λ estimates vary around the real value and always stay in the margin as the cell ages. Because the RUL prediction error increases or decreases as the λ estimation error, an accurate RUL prediction is thus ensured. This guarantee of high RUL prediction accuracy validates a high prediction stability of the BCT-based method for experimental data of lithium-ion batteries at different temperatures and current rates. The RUL prediction errors are within –20 to 10 cycles of most starting cycles of different cells. The STDs of the RUL prediction vary between 1.8 cycles and 7 cycles, and decrease as more training data is collected. The required amount of on-board data for accurate and precise RUL predictions is applicable for the lithium-ion battery RUL prediction for EVs. The battery life is generally designed to be as long as or longer than that of EVs, and the battery usually does not reach the EOL when EVs have been used for 60% of the designed lifetime. Therefore, when 60% of the on-board capacity data of lithium-ion batteries is collected, the developed method can be used to predict accurate and precise EOLs of batteries for EVs.

C. Remaining useful life prediction with offline training data

Figure 9 shows the RUL prediction results based on BCT when the offline capacity data is available, where the standard PF-based prognostic method [7] is also implemented as comparison. To eliminate the effects of cell inconsistencies, two or more offline cells should be utilized to initialize the model parameter of the online cell. Therefore, Cells A, C, and E are selected as the online cells because three offline samples' capacity data under each experimental condition is available. The initialized model parameter of the online cell based on BCT is the transformation parameter λ. Table 2 lists the λ reference values of different cells. Cells A, C, and E are considered online cells, whereas Cells A1-A3, C1-C3, and E1-E3 are considered offline cells under the same working conditions, respectively. It is observed that the λ reference of Cell A is larger than those values of other three cells including Cells A1-A3. The largest λ difference exists between those of Cells A and A1, which is –0.348 and falls within the proposed λ error margin in Section 5.1. The λ value of Cell C is the smallest among the four cells under the same experimental condition, and the difference between λ values of Cell C and Cell C1, which is the largest, is 0.547 and falls within the λ error margin. Cells E1 and E2,

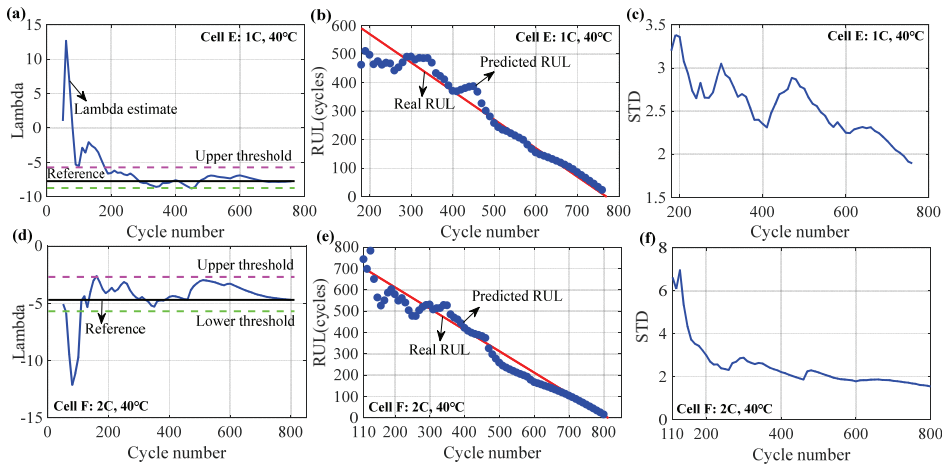

Fig. 8 Prediction results: (a) λ estimate of Cell E; (b) RUL prediction of Cell E; (c) STD of Cell E; (d) λ estimate of Cell F; (e) RUL prediction of Cell F; (f) STD of Cell F.

This article has been accepted for publication in a future issue of this journal, but has not been fully edited. Content may change prior to final publication. Citation information: DOI 10.1109/TIE.2018.2808918, IEEE Transactions on Industrial Electronics

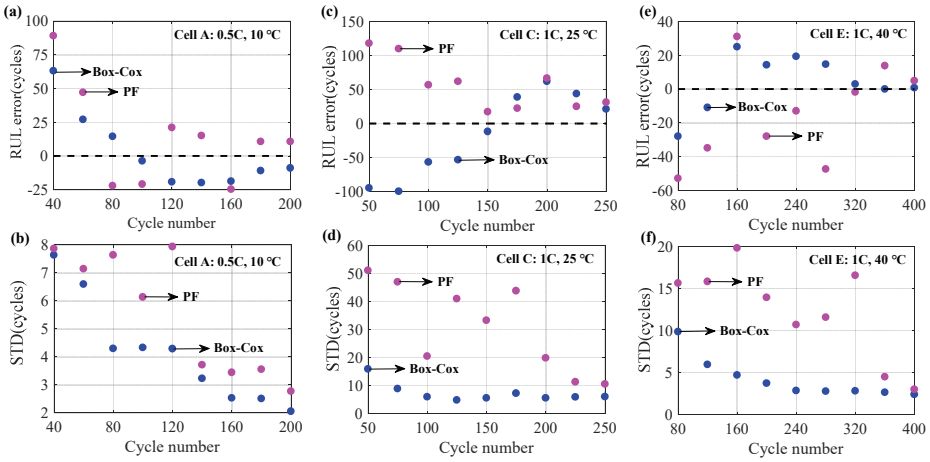

Fig. 9 RUL prediction results based on the BCT and the standard PF method: (a) RUL error of Cell A; (b) STD of Cell A; (c) RUL error of Cell C; (d) STD of Cell C; (e) RUL error of Cell E; (f) STD of Cell E.

respectively, have the largest and lowest λ values of –6.992 and –7.821 among the four cells. This λ difference is 0.829, which also falls within the λ error margin. The λ values of the offline cells under each working condition are averaged to obtain the λ estimate for the online cell. Therefore, the initialized λ values of Cells A, C, and E are, respectively, –2.461, –6.113, and –7.519. The λ estimation error of Cells A, C, and E are, respectively, –0.267, 0.421, and 0.212, which all fall within the λ error margin. A highly accurate RUL prediction can thus be ensured owing to the high prediction robustness of the BCT-based method against erroneous λ values. The standard PF-based method is implemented as Ref. [7], where a two-term exponential model is used to fit the offline degradation data. The fitted model parameters based on the capacity data of offline cells are fused using the Dempster–Shafer theory to initialize the model parameters for the online cell. Then the initialized aging model combined with the PF is further updated based on the available capacity data of the online cell for predicting its RUL at different cycles. The RUL prediction starts when 10% of the complete degradation data of the online cell is available and operates once 5% more capacity data is collected until 50% of the complete data. Table 3 lists the mean values of RUL prediction errors, in which the mean values of absolute RUL prediction errors and STDs for each cell are, respectively, listed.

Table 2: λ reference values of different cells

Label	λ value	Label	λ value	Label	λ value
Cell A	-2.194	Cell C	-6.534	Cell E	-7.731
Cell A1	-2.542	Cell C1	-5.987	Cell E1	-6.992
Cell A2	-2.456	Cell C2	-6.162	Cell E2	-7.821
Cell A3	-2.386	Cell C3	-6.185	Cell E3	-7.743

Figs. 9(a-b) show the RUL prediction results of Cell A, where the RUL prediction error is shown in Fig. 9(a) and the STD is shown in Fig. 9(b). Generally, the BCT predicts a more accurate and precise RUL than the PF method. Table 3 shows that the BCT-based mean value of absolute errors is 20.7 cycles, which is about 8 cycles smaller than that of the PF-based method. The BCT-based mean value of STDs is 4.2 cycles, whereas the PF-based mean value is 5.6 cycles. At 80 cycles, the BCT-based RUL prediction error and STD of Cell A are, respectively, 14 and 4.29 cycles, indicating an accurate and precise predicted RUL. Therefore, when some offline training data is available, only 20% of the compete degradation data of Cell A is required to predict an accurate and precise RUL by using the BCT method, whereas the PF method predicts an accurate and precise RUL at 140 cycles with a RUL prediction error and a STD being, respectively, 15 and 3.71 cycles. The comparison of the required online data by two methods indicates that another 60 cycles' capacity data, which occupies 15% of the complete capacity data of Cell A, is required by the PF method than the BCT method to predict an accurate and precise RUL.

Table 3: Mean value of RUL prediction errors

Method	Indicator	Cell A	Cell C	Cell E
BCT	Mean Absolute Error	20.7	53.7	10.6
	Mean STD	4.2	7.2	3.9
PF	Mean Absolute Error	29.0	56.5	22.0
	Mean STD	5.6	30.8	11.0

Figs. 9(c-d) show the RUL prediction results of Cell C. The absolute RUL prediction errors and STDs of Cell C based on PF are larger than those based on BCT, especially the STD values of the PF method, which are generally 10–40 cycles larger than those of the BCT method. Table 3 shows that the PF-based mean STD is about 23 cycles larger than that based on the BCT method. This low RUL prediction precision based on PF is mainly caused by the decreasing slope of capacity degradation as the battery ages and the low slope of capacity degradation at the battery EOL. Fig. 1 shows that the capacity degradation slope of Cell C is large at the beginning and decreases to a small value at the battery EOL as the cycle number increases. In this case, the nonlinear aging models with similar degradation trajectories can result in quite different RUL predictions. The transformed capacities using BCT share a linear degradation trend with the same capacity degradation rate, which can be observed in Fig. 3. In this case, the linear aging models with similar degradation trajectories result in similar RUL predictions, a more accurate and precise RUL is thus predicted than the PF-based method. The BCT method predicts an accurate and precise RUL at 150 cycles with a RUL prediction error and an STD being, respectively, –12 and 5.49 cycles. The PF method predicts precise RULs at 225 and 250 cycles, with the prediction STDs being, respectively, 11.22 and 10.43 cycles, and the RUL prediction errors at these two cycles are, respectively, 25 and 31 cycles. By balancing the RUL prediction accuracy and precision, the PF method predicts an accurate and precise RUL at 225 cycles, which is 75 cycles larger than that based on BCT. 75 cycles' data accounts for 15% of the complete data of Cell C, indicating 15% less online data is required by the BCT method than by the PF method.

Figs. 9(e-f) show the RUL prediction results of Cell E, where the BCT-based method predicts RUL with the mean absolute error and mean STD of RUL predictions being, respectively,

10.6 and 3.9 cycles, which are, respectively, about 10 and 7 cycles smaller than those based on the PF method. The BCT method predicts an accurate and precise RUL at 120 cycles, which occupies 15% of the complete capacity data of Cell E, and the prediction error and STD are, respectively, –11 and 5.95 cycles. The PF method predicts an accurate and precise RUL at 360 cycles, which occupies 45% of the complete data, with a prediction error and a STD being, respectively, 14 and 4.47 cycles. Therefore, 30% less capacity data, which amounts to 240 cycles' data, is required by the BCT than the PF for an accurate and precise predicted RUL for Cell E.

Based on the BCT method, when some offline data is available, the required online data accounts for 15%-30% of the complete data of the cell for an accurate and precise RUL prediction, whereas 15%-30% more online data is required by the PF method. The required cycles' data by the BCT method is 60-240 cycles smaller than that by the PF method to predict an accurate and precise RUL, which amounts to 1-3 months' acceleration aging test time. Note that the developed method is not limited to reducing the acceleration aging test time of lithium-ion batteries, and can be applied in cases when some offline training capacity data is available.

VI. Conclusions

The lithium-ion battery remaining useful life (RUL) prediction for electric vehicles (EVs), which ensures the battery functions reliably, has attracted more and more attention in recent years. The current RUL prediction techniques, which mainly depend on offline training data, are not applicable to the battery RUL prediction of EVs. It is difficult to design acceleration aging tests of lithium-ion batteries to simulate the dramatically changeable working conditions of EVs, and to collect effective offline training data. To address this problem, this paper developed an on-board lithium-ion battery RUL prediction method independent of offline training data.

In the developed method, the Box–Cox transformation (BCT) was used to transform the collected capacity data and to construct a linear model between the transformed capacities and cycles. The model parameters were identified using the least squares algorithm. The battery RUL prediction was obtained by the extrapolation of the linear model, and the prediction uncertainties were generated using the Monte Carlo (MC) simulation. To validate the RUL prediction performance of the developed method, experimental data covering 15 cells under three current rates including 0.5C, 1C, and 2C, and three temperatures including 10 ℃, 25 ℃, and 40 ℃ was collected.

The robustness of the developed method against erroneous transformation parameters λ was conducted. Experimental results show that an accurate and precise RUL can be predicted if the λ errors falls within [–1, 2], indicating a high prediction stability of the BCT-based method for battery RUL predictions. Experimental results show that when 15%-60% of the complete capacity data of the on-board cell is collected, the identified λ errors fall in the λ error margin [–1, 2]. The λ error varies within the error margin and converges to zero as more capacity data is collected so that an accurate and precise RUL prediction can be ensured. The battery RUL prediction errors and standard deviations (STDs) are, respectively, within [–20, 10] cycles and [1.8, 7] cycles. Note that the lithium-ion battery life of EVs is generally designed to be as long as or longer than that of EVs. Therefore, the battery RUL can be predicted using the developed method when EVs have been used 60% of the life time or longer to ensure an accurate and precise RUL prediction.

The developed method can also be performed based on offline training data so that the required online data can be reduced. Training data of three offline cells were used to initialize the model parameters of the online cell. Results show that an accurate and precise RUL can be predicted when only 15%-30% online data is collected, whereas for the particle filter (PF)-based method, the required online data doubles. This advantage of the developed method can be applied for reducing the acceleration aging test time of lithium-ion batteries, where three or more cells are generally experimented under each test condition. Experimental results show that when some offline training data is available, the required cycles' data by the developed method is 60-240 cycles smaller than that by the PF-based method, which amounts to 1-3 months' acceleration test time.

References

[1] Y. Z. Zhang, R. Xiong, H. W He, and W. X. Shen, "Lithium-ion battery pack state of charge and state of energy estimation algorithms using a hardware-in-the-loop validation," *IEEE Transactions on Power Electronics*, vol. 32, no. 6, pp. 4421–4431, Jun. 2017.

[2] S. Peng, C. Chen, H. Shi, and Z. Yao, "State of Charge estimation of battery energy storage systems based on adaptive unscented Kalman filter with a noise statistics estimator," *IEEE Access*, vol. 5, pp. 13202 – 13212, 2017.

[3] R. Xiong, Y. Zhang, H. He, X. Zhou, and M. Pecht, "A double-scale, particle-filtering, energy state prediction algorithm for lithium-ion batteries," *IEEE Transactions on Industrial Electronics*, vol. 65, no. 2, pp. 1526–1538, Feb. 2018.

[4] R. Xiong, J.Y Cao, Q. Q Yu, H. He and F.C. Sun, "Critical Review on the Battery State of Charge Estimation Methods for Electric Vehicles", *IEEE Access*, 2017, doi: 10.1109/ACCESS. 2017. 2780258.

[5] Y. Song, D. Liu, C. Yang, and Y. Peng, "Data-driven hybrid remaining useful life estimation approach for spacecraft lithium-ion battery," *Microelectronics Reliability*. 2017, DOI: 10.1016/j.microrel.2017.06.045.

[6] B. Saha, K. Goebel, S. Poll, and J. Christophersen, "Prognostics methods for battery health monitoring using a Bayesian framework," *IEEE Transactions on Instrumentation and Measurement*, vol. 58, no. 2, pp. 291–296, Feb. 2009.

[7] W. He, N. Williard, M. Osterman, and M. Pecht, "Prognostics of lithium-ion batteries based on Dempster–Shafer theory and the Bayesian Monte Carlo method," *Journal of Power Sources*, vol. 196, no. 23, pp. 10314–10321, Dec. 2011.

[8] Y. Xing, E. W. Ma, K. L. Tsui, and M. Pecht, "An ensemble model for predicting the remaining useful performance of lithium-ion batteries," *Microelectronics Reliability*, vol. 53, no. 6, pp. 811–820, Jun. 2013.

[9] Q. Miao, L. Xie, H. Cui, W. Liang, and M. Pecht, "Remaining useful life prediction of lithium-ion battery with unscented particle filter technique," *Microelectronics Reliability*, vol. 53, no. 6, pp. 805–810, Jun. 2013.

[10] Z. Liu, G. Sun, S. Bu, J. Han, X. Tang, and M. Pecht, "Particle learning framework for estimating the remaining useful life of lithium-ion batteries," *IEEE Transactions on Instrumentation and Measurement*, vol. 66, no. 2, pp. 280–293, Feb. 2017.

[11] X. Su, S. Wang, M. Pecht, L. Zhao, and Z. Ye, "Interacting multiple model particle filter for prognostics of lithium-ion batteries," *Microelectronics Reliability*, vol. 70, pp. 59–69, Mar. 2017.

[12] H. Dong, X. Jin, Y. Lou, and C. Wang, "Lithium-ion battery state of health monitoring and remaining useful life prediction based on support vector regression-particle filter," *Journal of Power Sources*, vol. 271, pp.114–123, Dec. 2014.

[13] X. Zheng, and H. Fang, "An integrated unscented kalman filter and relevance vector regression approach for lithium-ion battery remaining useful life and short-term capacity prediction," *Reliability Engineering and System Safety*, vol. 144, pp. 74–82, Dec. 2015.

[14] A. Nuhic, T. Terzimehic, T. Soczka-Guth, M. Buchholz, and K. Dietmayer, "Health diagnosis and remaining useful life prognostics of lithium-ion batteries using data-driven methods," *Journal of Power Sources*, vol. 239, pp.680–688, Oct. 2013.

[15] M. A. Patil, P. Tagade, K. S. Hariharan, S. M. Kolake, T. Song, T. Yeo, and S. Doo, "A novel multistage Support Vector Machine based approach for Li ion battery remaining useful life estimation," *Applied Energy*, vol. 159, pp. 285–297, Dec. 2015.

[16] D. Liu, J. Zhou, H. Liao, Y. Peng, and X. Peng, "A health indicator extraction and optimization framework for lithium-ion battery degradation modeling and prognostics," *IEEE Transactions on Systems, Man, and Cybernetics: Systems,* vol. 45, no. 6, pp. 915–928, Jun. 2015.

[17] J. Liu, A. Saxena, K. Goebel, B. Saha, and W. Wang, "An adaptive recurrent neural network for remaining useful life prediction of lithium-ion batteries," in *Proc. of Annual Conference of the Prognostics Health Management Society*, 2010, pp. 1–9.

[18] S. Watanabe, M. Kinoshita, and K. Nakura, "Capacity fade of $LiNi_{(1-x-y)}Co_xAl_yO_2$ cathode for lithium-ion batteries during accelerated calendar and cycle life test. I. Comparison analysis between $LiNi_{(1-x-y)}Co_xAl_yO_2$ and $LiCoO_2$ cathodes in cylindrical lithium-ion cells during long term

storage test," *Journal of Power Sources*, vol. 247, pp. 412–422, Feb. 2014.
[19] Y. Gao, J. Jiang, C. Zhang, W. Zhang, Z. Ma, and Y. Jiang, "Lithium-ion battery aging mechanisms and life model under different charging stresses," *Journal of Power Sources*, vol. 356, pp. 103–114, Jul. 2017.
[20] M. Dubarry, C. Truchot, M. Cugnet, B. Y. Liaw, K. Gering, S. Sazhin, D. Jamison, and C. Michelbacher, "Evaluation of commercial lithium-ion cells based on composite positive electrode for plug-in hybrid electric vehicle applications. Part I: Initial characterizations," *Journal of Power Sources*, vol. 196, pp. 10328–10335, Dec. 2011.
[21] M. Safari, and C. Delacourt, "Aging of a Commercial Graphite/LiFePO$_4$ Cell," *Journal of The Electrochemical Society*, vol. 158, no. 10, pp. A1123–A1135, 2011.
[22] G. E. P. Box and D. R. Cox, "An analysis of transformations," *Journal of the Royal Statistical Society. B*, vol. 26, no. 2, pp. 211–252, 1964.
[23] J. W. Osborne, "Improving your data transformations: Applying the Box–Cox transformation," *Practical Assessment, Research & Evaluation*, vol. 15, no. 12, pp. 1–9, 2010.
[24] D. C. Montgomery, E. A. Peck, and G. G. Vining, *Introduction to Linear Regression Analysis*, 5th ed. New York: Wiley, 2012.
[25] W. J. Conover, *Practical Nonparametric Statistics*, 3rd ed. New York: Wiley, 1999.
[26] C. L. T. Borges, and J. A. S. Dias, "A model to represent correlated time series in reliability evaluation by non-sequential Monte Carlo simulation," *IEEE Transactions on Power Systems*, vol. 32, no. 2, pp. 1511–1519, Mar. 2017.
[27] B. Zhang, L. Tang, J. DeCastro, and K. Goebel, "A verification methodology for prognostic algorithms," in *Proc. 2010 IEEE Autotestcon Conf.*, Orlando, FL, USA, Sep. 2010, pp. 1–8.
[28] M. Beer, and P. D. Spanos, "Neural network based Monte Carlo simulation of random processes," in *Proc. of the Ninth International Conference on Structural Safety and Reliability*, pp. 2179–2186, 2005.
[29] R. Dufo-López, I. R. Cristóbal-Monreal, and J. M. Yusta, "Stochastic-heuristic methodology for the optimisation of components and control variables of PV-wind-diesel-battery stand-alone systems," *Renewable Energy*, vol. 99, pp. 919-935, Dec. 2016.

Yongzhi Zhang (S'15) was born in Jiangsu, China, in January 1991. He received the B.S.degree in vehicle engineering from Chongqing University, Chongqing, China, in 2013. He is currently working toward the Ph.D. degree in mechanical engineering with the National Engineering Laboratory for Electric Vehicles, Beijing institute of Technology, Beijing, China.

He is currently a Research Scholar with the Center for Advanced Life Cycle Engineering, University of Maryland, College Park, MD, USA. His research interests include prognostics and health management of lithium-ion batteries.

Mr. Zhang received the Best Paper Awards in the International Symposium on Electric Vehicles, Sweden, 2017.

Rui Xiong (S'12–M'14–SM'16) received the M.Sc. degree in vehicle engineering and the Ph.D. degree in mechanical engineering from Beijing Institute of Technology, Beijing, China, in 2010 and 2014, respectively. He conducted scientific research as a joint Ph.D. student in the DOE GATE Center for Electric Drive Transportation at the University of Michigan, Dearborn, MI, USA, between 2012 and 2014.

Since 2014, he has been an Associate Professor in the Department of Vehicle Engineering, School of Mechanical Engineering, Beijing Institute of Technology, Beijing, China. Since 2017, he has been an Adjunct Professor in the Faculty of Science, Engineering and Technology, Swinburne University of Technology, Melbourne, Australia. He has conducted extensive research and authored more than 100 peer-reviewed articles. He holds eight patents. His research interests mainly include electrical/hybrid vehicles, energy storage, and battery management system.

Dr. Xiong received the Excellent Doctoral Dissertation from Beijing Institute of Technology in 2014, the first prize of Chinese Automobile Industry Science and Technology Progress Award in October 2015 and the second prize of National Defense Technology Invention Award in December 2016. He received Best Paper Awards from the journal Energies and several International conferences by four times. He is serving as the Associate Editors of IEEE Access and Energy-Ecology and Environment (E3), Editorial Board of the Energies, Sustainability, Vehicles and Batteries, subject assistant editor of Applied Energy, and Guest editor of the Journal of Cleaner Production. He was the conference chair of the 2017 International Symposium on Electric Vehicles (ISEV2017) hold in Stockholm, Sweden.

Hongwen He (M'03–SM'12) received the Ms.E. degree from the Jilin University of Technology, Changchun, China, in 2000 and the Ph.D. degree from the Beijing Institute of Technology, Beijing, China, in 2003, both in vehicle engineering.

He is currently a Professor with the National Engineering Laboratory for Electric Vehicles, School of Mechanical Engineering, Beijing Institute of Technology. He has published more than 100 papers and holds 20 patents. His research interests include power battery modeling and simulation on electric vehicles, design, and control theory of the hybrid power trains.

Dr. He was recipients of the second prize of Chinese National Science and Technology Award for the work on the development of new-energy electric bus powertrains in 2015, the first prize of Henan Science and Technology Award for the work on the development of hybrid bus powertrain in 2013.

Michael G. Pecht (S'78–M'83–SM'90–F'92) received the B.S. degree in physics in 1976, the M.S. degree in electrical engineering in 1978, and the M.S. and Ph.D. degrees in engineering mechanics from the University of Wisconsin-Madison, Madison, WI, USA, in 1979 and 1982 respectively.

He is the Founder and Director of the Center for Advanced Life Cycle Engineering, University of Maryland, College Park, MD, USA, which is funded by over 150 of the world's leading electronics companies at more than US$6M/year. He is also a Chair Professor of mechanical engineering and a Professor of applied mathematics, statistics, and scientific computation with the University of Maryland. He has written more than 20 books, 400 technical articles, and has eight patents.

Dr. Pecht is a Professional Engineer, a Fellow of the American Society of Mechanical Engineers, a Fellow of the Society of Automotive Engineers, and a Fellow of the International Microelectronics Assembly and Packaging Society. He is the Editor-in-Chief of the IEEE ACCESS, and served as the Chief Editor of the IEEE TRANSACTIONS ON RELIABILITY for nine years and the Chief Editor for the Microelectronics Reliability for 16 years. He has also served on three U.S. National Academy of Science studies, two U.S. Congressional investigations in automotive safety, and as an expert to the U.S. Food and Drug Administration.